

RESEARCH ARTICLE OPEN ACCESS

# Metamer Mismatching Predicts Color Difference Ellipsoids

Emitis Roshan | Brian Funt

School of Computing Science, Simon Fraser University, Vancouver, Canada

**Correspondence:** Brian Funt ([funt@sfu.ca](mailto:funt@sfu.ca))

**Received:** 11 December 2023 | **Revised:** 3 October 2024 | **Accepted:** 9 December 2024

**Funding:** This work was supported by Natural Sciences and Engineering Research Council of Canada.

**Keywords:** color difference metrics | color discrimination | discrimination ellipsoids | metamer mismatching

## ABSTRACT

It is well known that color-discrimination thresholds vary throughout color space, as is easily observed from the familiar MacAdam ellipses plotted in chromaticity space. But why is this the case? Existing formulations of uniform color spaces (e.g., CIELAB, CIECAM02, CAM16-UCS) and their associated color-difference DE metrics are all models, not theories, based on fits to psychophysical data. While they are of great practical value, they provide no theoretical understanding as to why color discrimination varies as it does. In contrast, the hypothesis advanced and tested here is that the degree of color variability created by metamer mismatching is the primary (although not exclusive) factor underlying the variation in color-discrimination thresholds throughout color space. Not only is it interesting to understand the likely cause of the variation, but knowing the cause may foster the development of more accurate color difference metrics.

## 1 | Introduction

In the past, numerous experiments have been conducted to measure color-discrimination thresholds for different colors. Surface materials such as painted ceramic, fabric, printed samples, paint, and also CRT or LCD display colors were used in various experiments [1–7]. The experimental data show that the color-discrimination threshold varies as a function of the color involved. Many color spaces or color difference formulas have been developed to fit the experimental data [8–12]. Sophisticated appearance models have been designed with their parameters optimized to fit the existing data [13–20], but the underlying cause of the variation in color-discrimination thresholds is not well understood. Recently, Funt et al. [21] showed that metamer mismatching provides a plausible explanation for the way in which color difference sensitivity, as represented by the size of discrimination ellipsoids, depends on where the colors reside within color space. This metamer-mismatching-based approach is further explored here to show that the degree of metamer mismatching explains and predicts not only the volume of a given

color's discrimination ellipsoid but also its dimensions and orientation as well.

Given a surface reflectance resulting in a given cone response triple under a given light, many other different surface reflectances will produce the same cone response triple under that same light. Such reflectances are called metamers. However, the tristimulus values of these metamers may no longer match (i.e., they mismatch) under a different light. This phenomenon is referred to as “illuminant-induced metamer mismatching”. The set of all tristimulus values of all possible metameric reflectances under a second light constitutes a convex set known as the metamer mismatching body (MMB henceforth). Color difference thresholds and suprathresholds are usually represented by ellipses in 2D chromaticity planes or by ellipsoids in 3D color spaces. As shown by Funt et al. [21], the normalized MMB volume has an inverse relationship to the volume of color-discrimination ellipsoid. Their hypothesis is that the MMB volume reflects the uncertainty in distinguishing a color from a very similar color since the MMB volume is a

This is an open access article under the terms of the [Creative Commons Attribution-NonCommercial](https://creativecommons.org/licenses/by-nc/4.0/) License, which permits use, distribution and reproduction in any medium, provided the original work is properly cited and is not used for commercial purposes.

© 2025 The Author(s). *Color Research & Application* published by Wiley Periodicals LLC.

measure of how different the metameric reflectance functions can be. Thus, to overcome this uncertainty, the visual system has become more sensitive for colors having larger MMBs in order to distinguish them from their metamers. As a result, discrimination ellipsoids are the smallest near gray where the MMB volumes are the largest. Statistical tests on four sets of experimental data (Funt et al. [21]) show that predictions of ellipsoid volumes based on the metamer mismatching hypothesis are as accurate on average as those of CAM16-UCS [13, 14], even though CAM16-UCS is based on direct fits to similar experimental data.

The results reported below extend the use of the metamer mismatching hypothesis beyond predicting only the volume of a given color's color-discrimination ellipsoid and show how the normalized MMB can be used to predict, not only the ellipsoid's volume but also the ellipsoid's dimensions and orientation as well. This provides further evidence that metamer mismatching underlies the variation in color discrimination throughout color space.

## 2 | Background

Color-discrimination thresholds and color appearance models that provide uniform color spaces are closely linked topics. CAM16 is one of the most recent color appearance models, obtained by optimizing a  $3 \times 3$  matrix to replace the CAT02 and HPE matrices of the CIECAM02 model to better fit the experimental data. The lightness, colorfulness, and hue attributes have themselves been modified in a nonlinear fashion in the definition of an improved CIELAB-like uniform color space called CAM16-UCS. The original CIELAB is a device-independent color space based on the opponent color model of human vision. Unlike CAM16-UCS, it does not take any appearance phenomena into account, other than the white point. Nevertheless, CIELAB is extensively used in the industry as it is less complicated and computationally simpler than CAM16-UCS.

Despite the advances in color appearance models and the uniformity in their corresponding color spaces, the Euclidean distance in CIELAB color space is widely used as the just noticeable

difference (JND) in several studies. MacAdam [22] showed that the JNDs are proportional to the standard deviation of color matchings, meaning the ellipsoids fitted to the discrimination data represent the JNDs in different directions. Mahy et al.'s [23] evaluation of uniform color differences offered an average value of  $DE_{ab} = 2.3$  for the JND in CIELAB space. Martin et al. [24] utilize color information in scan matching, a particular aspect of mapping in the simultaneous localization and mapping (SLAM) problem. A change in the orientation between scans causes failure in the matching process for mobile robots. A  $DE_{ab}$  of 2.3 is used in their study to detect a noticeable color transition. Hao et al. [25] introduced a method to hide a binary image in the gradient domain of a host image. They considered a Euclidean  $DE_{ab}$  of 2.3 as the JND to make sure the embedded data are imperceptible. Zhang et al. [26] proposed a real-time rendering scheme for laser-beam-scanning-optical-see-through, head-mounted displays. In their method, the colors of the virtual content on the display are optimized based on the background color while keeping the difference between the original and optimized colors under  $2.3 DE_{ab}$ .

## 3 | Color-Discrimination Ellipsoid Prediction

Funt et al. [21] show that for the color centers with larger normalized MMBs, the color-discrimination ellipsoids are smaller and vice versa. The MMBs are normalized by  $C^3$ , the cube of the Euclidean distance,  $C$ , from the origin to the given color center. The inverse relationship between the normalized MMB volume ( $MMB_{vol} / C^3$ ) and the discrimination ellipsoid volume ( $E_{vol}$ ) is demonstrated by the strong correlation coefficient between  $C^3 / MMB_{vol}$  and  $E_{vol}$ . The question naturally arises as to whether or not there is a similar inverse relationship between a normalized MMB and the shape of the corresponding discrimination ellipsoid.

To model the general shape of an MMB, we use its equivalent ellipsoid (EE henceforth) as described in Roshan et al. [27]. An MMB's EE is an ellipsoid that has the same moments of inertia (i.e., inertia tensor) as the MMB. The moments of inertia are calculated based on the MMB being a three-dimensional solid of uniform density, and the EE's moments describe the radii and

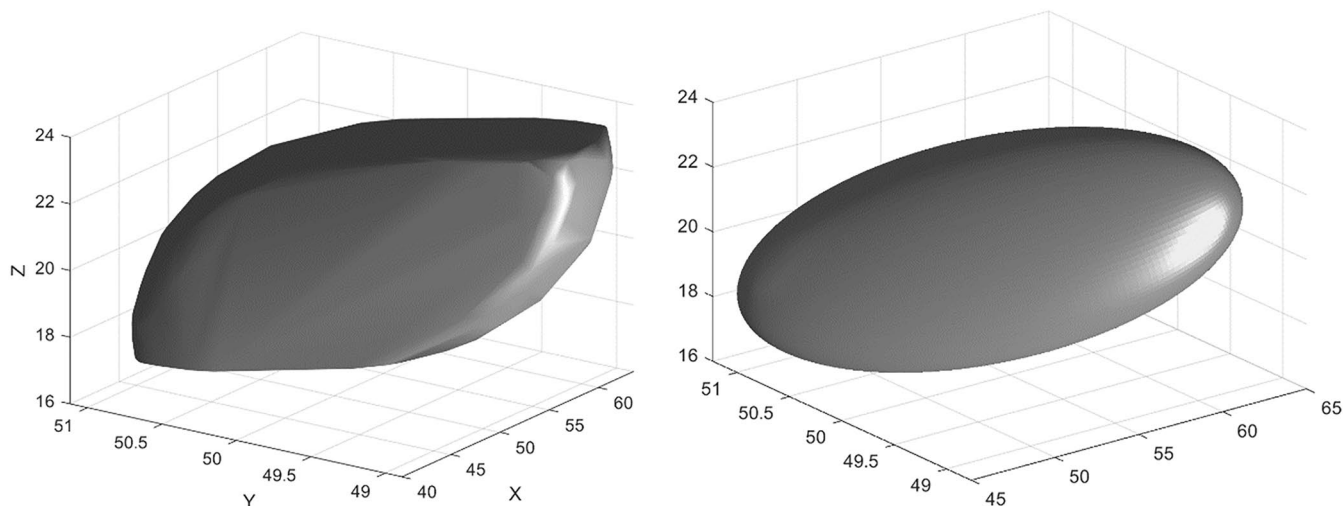


**FIGURE 1** | A sample MMB for the gray color center on the left and its EE on the right.

principal axes of the EE and represent its dimensions and orientation, respectively. A typical MMB and its EE are shown in Figure 1.

Given an MMB, let the radii of its EE be  $r_1$ ,  $r_2$ , and  $r_3$ . Because of the strong correlation coefficients between  $C^3/MMB_{vol}$  and  $E_{vol}$ , it is reasonable to expect the ellipsoid with the radii  $C/r_1$ ,  $C/r_2$ , and  $C/r_3$  to be similar to those of the corresponding discrimination ellipsoid. However, the orientation of the MMB, and consequently its EE, depends on the choice of the second illuminant. This orientation dependence needs to be modeled as well, as described below.

The MMBs are computed for the CIE 10° standard observer for a shift from CIE illuminant D65 to CIE A using the algorithm of Logvinenko et al. [28]. D65 is used as the first illuminant because the color centers and color-discrimination thresholds in the available experimental datasets are all measured and reported under D65. However, how should the second illuminant be chosen? In terms of predicting ellipsoid volumes, the second illuminant has little effect on the results as shown in Table 1.

However, the choice of the second illuminant does affect the MMB's orientation and hence the prediction of the corresponding ellipsoid's orientation. Figure 2 shows the EEs of three MMBs computed by going from (i) D65 to Horizon, (ii) D65 to U30, and (iii) D65 to CWF. The ellipsoids are translated to the origin, and their sizes are normalized. The long, medium, and short axes of each ellipsoid are shown with red, green, and blue lines, respectively. It is clear from Figure 2 that the orientation of the MMB, and consequently its EE, changes considerably with the second light. Clearly, the orientation needs to be standardized in some way.

The hypothesis proposed by Funt et al. [21] is that the metamer mismatching volume reflects the ambiguity in the nature of the underlying surface reflectance function. To see how this relates to how discrimination thresholds vary with

direction, consider that the MMB volume reveals how varied the reflectances are that result in the same color signal under a given illuminant. Given two color signals, the larger the intersection of their corresponding MMBs, the more varied is the set of reflectances that are metameric to both color signals. Therefore, the intersection of the MMBs indicates the degree of uncertainty, that is, the possibility of confusing their underlying surface reflectances. To the extent that this intersection varies with direction from the given color center, P, a human observer must be more sensitive to the colors in a direction creating significant uncertainty and less sensitive to the colors in directions of less uncertainty.

Although the intersection of the MMBs of two color signals signifies how likely it is to confuse their surface reflectances, the MMB orientation, and hence its overlap with other MMBs, varies with the choice of the second illuminant and needs to be normalized with respect to it. Also, the wing-like shape of the MMB can make the overlap computation very sensitive to the boundary point computation, especially near the tips. So, to compute the MMB intersection volumes, we suggest (1) using the EE of the MMB and (2) rotating the EEs of the MMBs to be aligned with the object-color solid (OCS) under D65 to cancel the rotation created by the second illuminant.

To integrate the observation that a human observer must be more sensitive to the colors in the directions of significant uncertainty, and less sensitive to the colors in the directions of less uncertainty, we begin by computing the MMB intersection in 14 different directions around each color center. The 14 vector directions are selected in the same way that Berns et al. [29] selected the vectors to measure the color difference tolerance in their experiment except that in our case, the vectors are defined in CIE XYZ space instead of CIELAB. The 14 vectors are plotted in Figure 3.

**TABLE 1** | The correlation coefficients between  $C^3/MMB_{vol}$  and  $E_{vol}$ , and the mean Jackknife estimates as a function of the second illuminant used in predicting ellipsoid volumes.

Second illuminant	Correlation coefficient	Mean Jackknife estimate
Horizon 2300 K	0.84	0.84
A 2800 K	0.83	0.83
U30 3000 K	0.90	0.90
TL84 3800 K	0.91	0.91
CWF 4100 K	0.89	0.89
F2 4230 K	0.89	0.89
F8 5000 K	0.9	0.9
F11 4000 K	0.9	0.9
C 6774 K	0.88	0.88

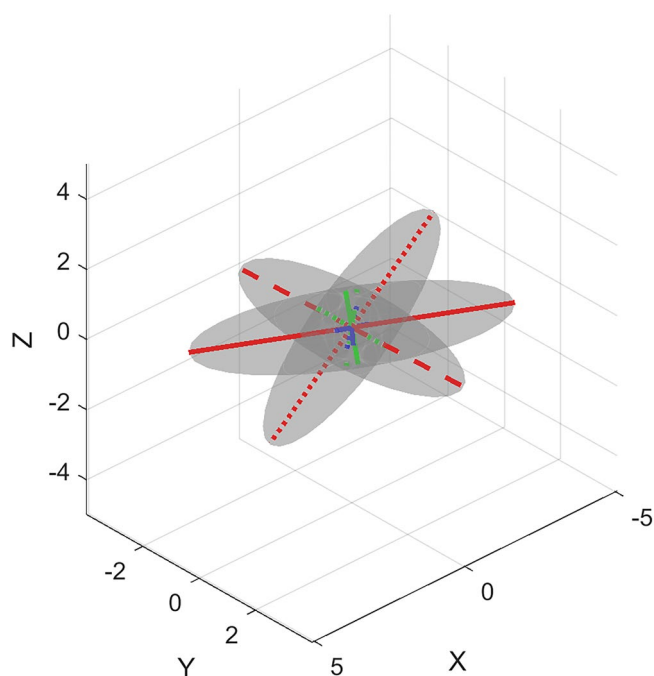


**FIGURE 2** | Three ellipsoids representing the MMB orientations computed by going from D65 to Horizon, D65 to U30, and D65 to CWF.

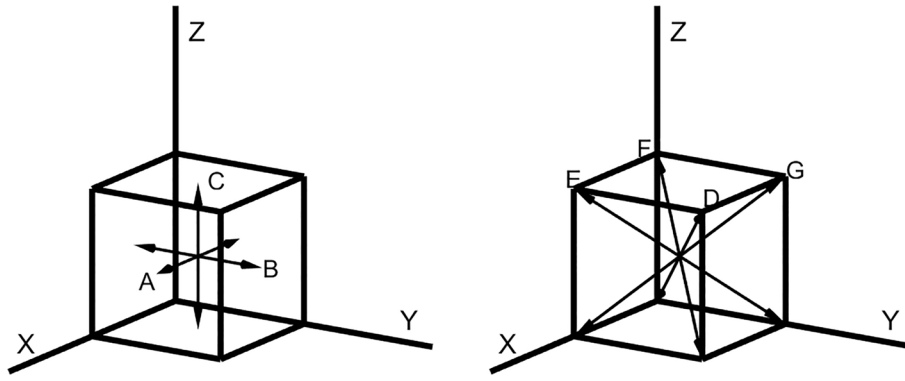


**FIGURE 3** | The 14 directions (vectors A, B, C, D, E, F, and G, and their reverse directions) are defined in CIE XYZ color space. Specifically,  $A = [1, 0, 0]$ ,  $B = [0, 1, 0]$ ,  $C = [0, 0, 1]$ ,  $D = [1, 1, 1]$ ,  $E = [1, -1, 1]$ ,  $F = [-1, -1, 1]$ , and  $G = [-1, 1, 1]$ .

Assuming the norm of the vector directions to be equal to 0.1 with their tails on a color center  $P$ , the tips/heads of the vectors define 14 neighboring colors around  $P$ . The MMBs for these 14 color neighbors plus one for the color center  $P$  are computed by going from D65 to illuminant A. The EEs of the 15 MMBs are computed and rotated to be aligned with the D65 OCS. Importantly, the length of each of these vectors is then computed as the volume of the intersection of the two EEs corresponding to the two colors at the tail and head of each vector. The tips of the new vectors (the same vector directions but with lengths equal to the overlap volumes) are used to fit an ellipsoid around  $P$  using the algorithm explained by Brown and MacAdam [30] color signals in that direction, so a human observer must be more sensitive in that direction to be able to distinguish the colors, and consequently the discrimination threshold becomes smaller.

The proposed method (see Figure 4) is as follows:

1. Given a color center,  $P$ , in CIE XYZ space, compute the MMB for an illuminant change from D65 to A.
2. Compute the EE of the MMB as proposed by Roshan et al. [27] and summarized above. Call it  $EE_P$ . The radii  $(r_1, r_2, r_3)$  from the longest to the shortest along with their corresponding axes  $(V_1, V_2, V_3)$  of the EE represent the lengths and directions of the principal axes of the MMB, respectively.
3. Compute the CIE D65 OCS for the standard observer ( $2^\circ$  or  $10^\circ$  depending on the test dataset) and CIE illuminant D65 using the two-transition optimal color reflectances as defined by Logvinenko [31]. Modeling the CIE D65 OCS as a rigid body of unit density, compute its EE and principal axes.
4. Compute the 14 color signals around  $P$  using the 14 vector directions plotted in Figure 3. Call these 14 neighboring color signals  $N_1$  to  $N_{14}$ . Compute the MMB for each of these color signals for a change from D65 to A.
5. Compute the EEs of the 14 MMBs. Call them  $EE_{N_1}, \dots, EE_{N_{14}}$ .
6. Rotate each of the 15 ellipsoids,  $EE_{N_1}, \dots, EE_{N_{14}}$  and  $EE_P$  to align with the principal axes of the D65 OCS.

7. Set the length of each vector equal to the volume of the intersection of the two ellipsoids for the two colors  $P$  and  $N_i$  at the tail and head of the vector.
8. Using the algorithm described by Brown and MacAdam [30], fit an ellipsoid to the 14 color signals located at the tips of the length-adjusted vectors from the previous step. Call the axes of this ellipsoid from the longest to the shortest  $(V'_1, V'_2, V'_3)$ .
9. Compute  $C$  as the Euclidean distance between the color center  $P$  and the origin. Scale the axes of  $EE_P$  such that their lengths  $(r_1, r_2, r_3)$  become  $(C/r_1, C/r_2, C/r_3)$ , respectively. Now, the order is reversed, with  $C/r_1$  being the shortest and  $C/r_3$  being the longest. Let the new axis vectors be  $(W_1, W_2, W_3)$ .

Rotate the size-adjusted ellipsoid defined by  $(W_1, W_2, W_3)$  such that its axes align with  $(V'_1, V'_2, V'_3)$ , respectively. The new size-adjusted and rotated ellipsoid is then the predicted discrimination ellipsoid for color center  $P$ .

#### 4 | Ellipsoid Similarity Measures

To evaluate the metamer mismatching hypothesis, an ellipsoid similarity measure is needed to compare the predicted ellipsoids to those derived from the psychophysical data. Moshtaghi et al. [32] proposed an ellipsoid similarity metric referred to as compound similarity (CS) for ellipsoid clustering and anomaly detection in wireless sensor networks. Their metric consists of three exponential factors representing the difference in the location, orientation, and dimensions of the ellipsoid pair. It is defined as

$$CS = e^{-\|\mu_1 - \mu_2\|} e^{-\|\sin\theta\|} e^{-\|\alpha^* - \beta^*\|} \quad (1)$$

The first component represents the positional similarity, where the exponent  $\|\mu_1 - \mu_2\|$  measures the Euclidean distance between the centers of the ellipsoids. The  $\sin\theta = (\sin\theta_1, \sin\theta_2, \sin\theta_3)$  in the second term measures the  $\sin$  of the angles between the associated eigenvector pairs. The symbols  $\alpha^* = (\alpha_1^*, \alpha_2^*, \alpha_3^*)$  and  $\beta^* = (\beta_1^*, \beta_2^*, \beta_3^*)$  represent the radii of the ellipsoids from the longest to the shortest. Since both predicted and experimental ellipsoids are centered at the same point, the first term is always

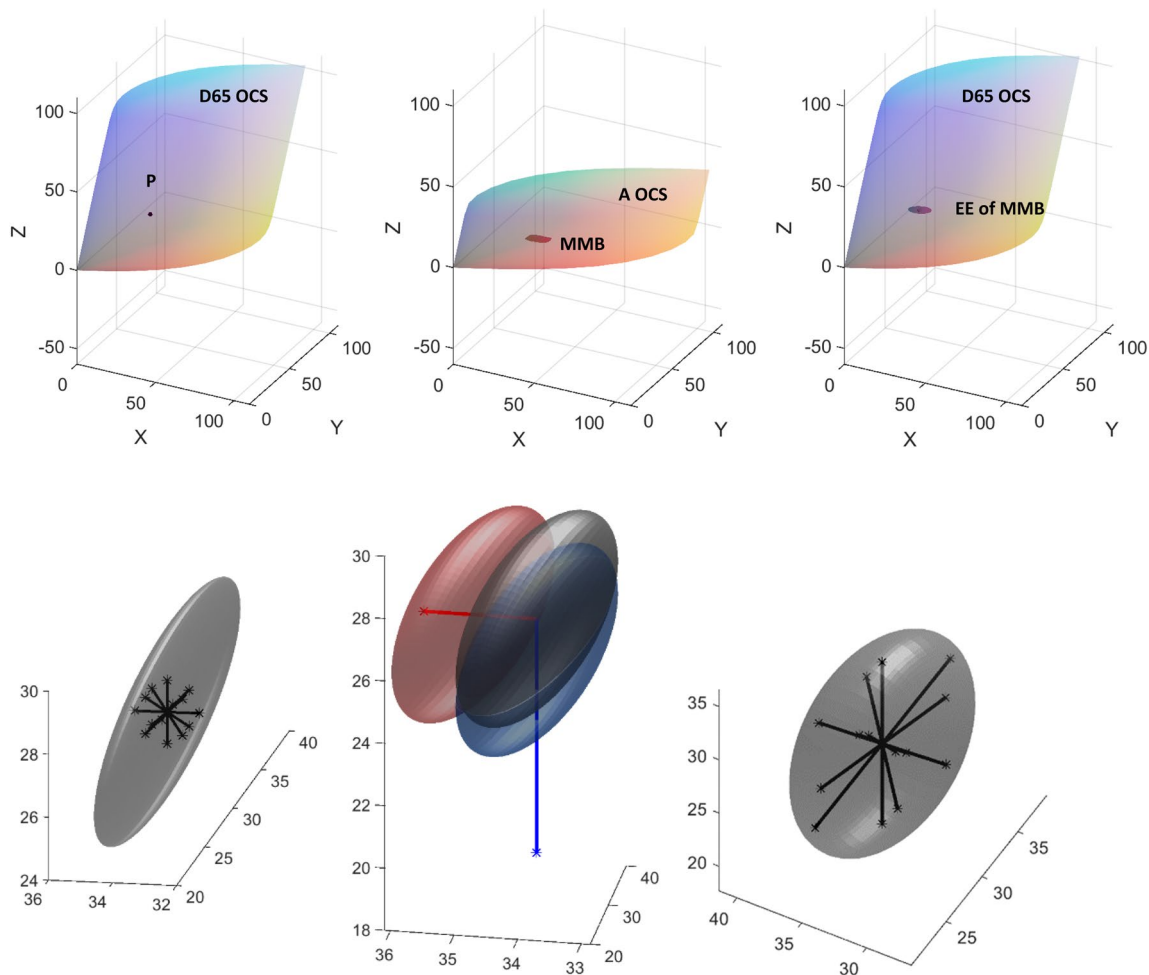


**FIGURE 4** | Illustration of the proposed algorithm: top left: D65 OCS and an arbitrary color center P within the OCS; top middle: the MMB for color center P for a change from illuminant D65 to A. The MMB is located inside the OCS for CIE illuminant A; top right: the EE of the MMB is calculated and then translated such that its centroid coincides with color center P within the D65 OCS; bottom left: the 14 vectors defined in Figure 3 are centered at P within the EE of the MMB; and the tips of the vectors (shown as black asterisks) indicate the N1 to N14 color signals around P; bottom middle: the EE of the MMB for P is shown in gray, with the EEs of the MMBs for two example color centers N2 and N10 shown in red and blue, respectively. The length of the N2 vector is adjusted to be equal to the overlap volume of the N2 EE and the P EE. The length-adjusted vector is shown in bright red. The length of the N10 vector (the blue line) is also adjusted to be equal to the overlap volume of the N10 and P EEs; bottom right: the length-adjusted vectors (black lines centered at P) are then used to fit an ellipsoid. The principal axes of the fitted ellipsoid are used as the principal axes of the predicted discrimination ellipsoid.

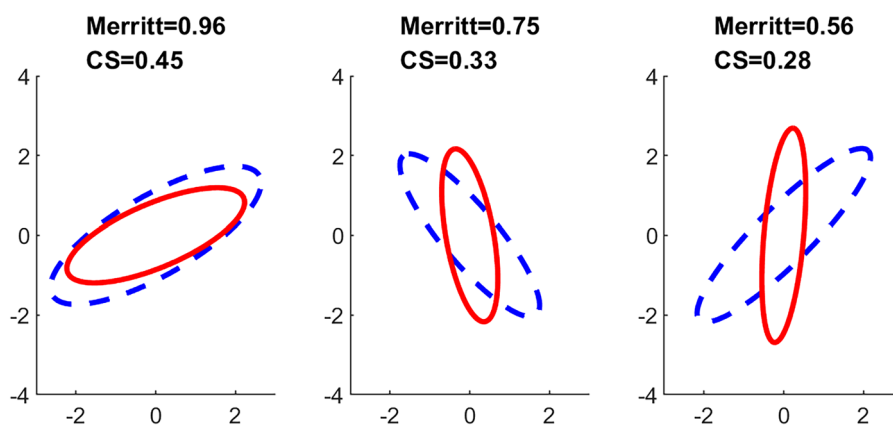


**FIGURE 5** | Merritt correlation coefficient and compound similarity (CS) measures for sample pairs of ellipses.

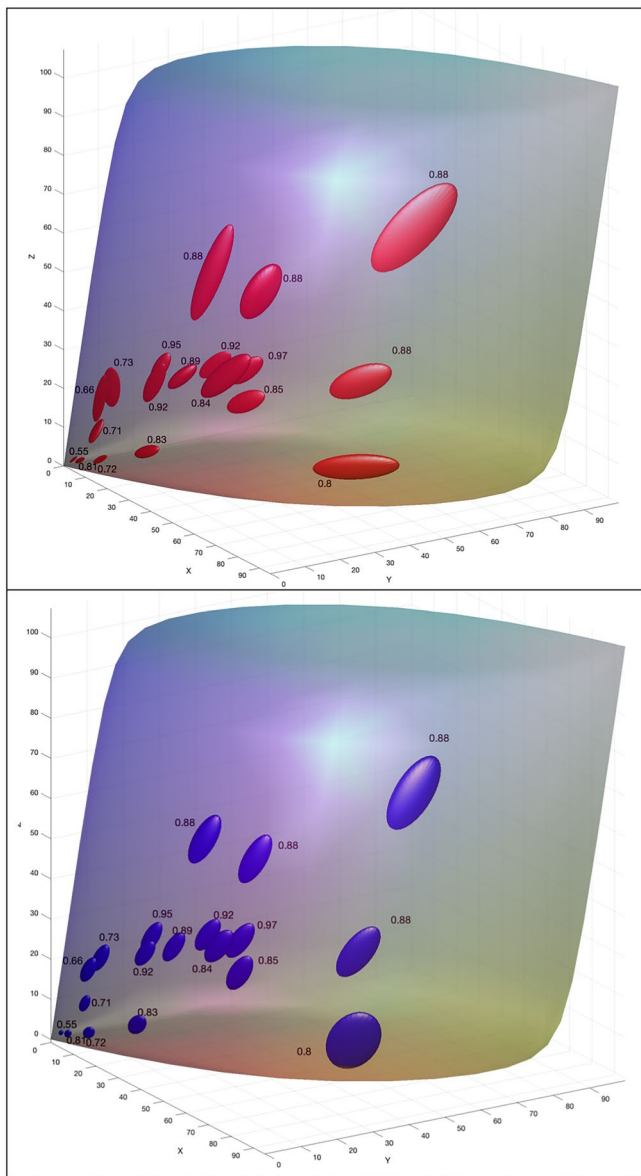


**FIGURE 6** | Experimental (top) and MMB-based (bottom) ellipsoids shown inside the OCS boundary labeled with the Merritt correlation coefficient between the corresponding ellipsoids.

equal to zero; hence, it is only the angles between their major axes and the difference in their lengths that matter. The value of the CS metric can vary between 0 and 1, with 1 indicating two identical ellipsoids.

Another metric, proposed by Merritt [33], is based on computing the overlap between two Gaussian distributions. Since both the experimental and predicted ellipsoids are centered at the same color center, only the shape and rotational similarities are relevant. Each ellipsoid can be described by a symmetric  $3 \times 3$  matrix,  $U$ , such that its eigenvectors represent the axes, and the inverses of the square root of the eigenvalues represent their lengths. Matrix  $U$  can be regarded as the covariance matrix of a Gaussian distribution. Let  $U$  and  $V$  be the covariance matrices corresponding to two ellipsoids. The Merritt correlation is then defined as

$$Merritt(U, V) = \frac{[\det(U^{-1})\det(V^{-1})]^{1/4}}{[1/8\det(U^{-1} + V^{-1})]^{1/2}} \quad (2)$$

The closer the value to 1, the more similar the ellipsoids. Sample pairs of ellipses with their similarity measures are plotted in Figure 5.

## 5 | Results

Since metamer-mismatching-based prediction is based on the MMBs of surface colors, only the experimental discrimination ellipsoids measured using physical color patches (i.e., not colors on a display or created from a mixture of lights) are useful for testing the accuracy of the proposed model of color discrimination. Berns et al. [29] prepared color samples by spraying acrylic-lacquer automotive coating onto primed aluminum panels and measured the color difference data for 19 color centers. The result is known as the RIT\_DuPont dataset. Melgosa et al. [34] derived discrimination ellipsoids from that data.

For the CIE reference color centers recommended by Roberston [35], Witt [36] acquired data for four of them using painted

**TABLE 2** | Ellipsoid similarity measures between the experimental ellipsoid versus MMB-based ellipsoid prediction, and experimental ellipsoid versus CIELAB and CAM16\_UCS ellipsoid predictions.

	MMB-based prediction using MMB overlap volume		CIELAB Ellipsoid prediction using unit $\Delta E$ spheres		CAM16-UCS Ellipsoid prediction using unit $\Delta E$ spheres	
	Merritt CC	Compound similarity	Merritt CC	Compound similarity	Merritt CC	Compound similarity
Melgosa	0.83	0.41	0.85	0.44	0.93	0.53
Huang	0.82	0.36	0.77	0.33	0.87	0.43
Cheung	0.81	0.37	0.82	0.38	0.89	0.41
Witt	0.82	0.55	0.83	0.62	0.93	0.73
Mean over all	0.82	0.40	0.81	0.41	0.90	0.50

samples, and Cheung [37] acquired data for five of them (four centers in common with Witt plus an additional one) using dyed wool fabric. Huang et al. [38] used a printer to generate color patches around the 17 CIE color centers.

The algorithm of Logvinenko et al. [28] is used to compute the MMBs for the change of illuminant from D65 to A for each of the color centers used in the experiments described above. Since the theoretical MMBs are based on five-transition, zero-one theoretical reflectances, they will be larger than the typical MMB in practice. Zhang et al. [39] showed that the MMBs of reflectances found in practice followed the same trends as those of the theoretical reflectances. They reported: “Based on a set of over 25 million spectral reflectances of real objects, estimates of the size of the potential metamer mismatch bodies were computed for the color signals generated from 5,069 test reflectances under 10 different illumination conditions. The average volumes of these empirically determined bodies were compared to the average volumes of the corresponding theoretically determined bodies and found to be roughly proportional but significantly smaller.” Zhang et al. [39] (p. A246). Given the theoretical MMBs, their EEs are calculated and then the algorithm explained above in Section III is used to predict the experimental ellipsoids. For comparison, a unit  $\Delta E_{ab}$  sphere is computed in CIELAB around each color center and converted to CIE XYZ, where it becomes an ellipsoid. Figure 6 compares the predicted versus the experimental ellipsoids.

The mean similarity measures between the MMB-based predicted ellipsoids and the experimental data compared to the mean similarity between the ellipsoids resulting from unit  $\Delta E$  spheres in CIELAB and the experimental data for each dataset are reported in the first two columns of Table 2. On inspection of the table, it is clear that the accuracy of the two methods is equivalent.

The results in the third column of Table 2 are based on unit spheres in CAM16-UCS. Although CAM16-UCS fits the experimental data better than do either of the other two methods, it is not a fair comparison since CAM16-UCS is a modification of CAM16, which is based on a direct fit to much of the same experimental data. In machine-learning terms, the “training” and “test” sets are effectively the same.

## 6 | Conclusion

The results in Table 2 show that MMB-based prediction based only on the hypothesis that the uncertainty created by metamer mismatching underlies the variation in difference thresholds is as accurate as the CIELAB-based prediction. This is not to say that the proposed hypothesis is the sole explanation for the way color-discrimination thresholds vary as a function of the color involved. Noise and possibly some other factors may play a minor role. However, the strong correlation coefficients between the shape and orientation of the predicted ellipsoids and the experimental data support the fundamental premise that the uncertainty created by metamer mismatching explains why color discrimination varies throughout color space as it does. Such an understanding of why color discrimination varies as it does provides a theoretical underpinning for future work on color discrimination and uniform color spaces.

## Author Contributions

Both authors participated in the formulation of the proposed theory and algorithms, and in writing and editing of the paper.

## Conflicts of Interest

The authors declare no conflicts of interest.

## Data Availability Statement

Data sharing not applicable to this article as no datasets were generated or analysed during the current study.

## References

1. S. S. Guan and M. R. Luo, “A Colour-Difference Formula for Assessing Large Colour Differences,” *Color Research and Application* 24 (1999): 344–355.
2. M. R. Pointer and G. G. Attridge, “Some Aspects of the Visual Scaling of Large Colour Differences,” *Color Research and Application* 22 (1997): 298–307.
3. S. M. Newhall, “Preliminary Report of the O.S.A. Subcommittee on the Spacing of the Munsell Colors,” *Journal of the Optical Society of America* 30 (1940): 617–645.
4. S. Badu, *Large Colour Differences Between Surface Colours*. Ph. D. thesis (Bradford, England: University of Bradford, 1986).
5. D. L. MacAdam, “Uniform Color Scales,” *Journal of the Optical Society of America* 64 (1974): 1619–1702.
6. S. Y. Zhu, M. R. Luo, and G. Cui, “New Experimental Data for Investigating Uniform Colour Spaces,” in *The 9th Congress of the International Colour Association* (AIC Color 2001), June 24–29 (Rochester, New York: International Colour Association, 2001), 626–629.
7. G. Wyszecki and G. Fielder, “New Color-Matching Ellipses,” *Journal of the Optical Society of America* 61, no. 9 (1971): 1135–1152.
8. G. Wyszecki, “Matching Color Differences,” *Journal of the Optical Society of America* 55, no. 10 (1965): 1319–1324.
9. J. Romero, J. A. García, L. J. del Barco, and E. Hita, “Evaluation of Color-Discrimination Ellipsoids in Two-Color Spaces,” *Journal of the Optical Society of America. A* 10, no. 5 (1993): 827–837.
10. A. Yebra, J. Garcia, J. Nieves, and J. Romero, “Chromatic Discrimination in Relation to Luminance Level,” *Color Research & Application* 26, no. 2 (2001): 123–131.
11. S. Wen, “A Color Difference Metric Based on the Chromaticity Discrimination Ellipses,” *Optics Express* 20, no. 24 (2012): 26441–26447.
12. G. Sharma, W. Wu, and E. N. Dalal, “The CIEDE2000 Color-Difference Formula: Implementation Notes, Supplementary Test Data, and Mathematical Observations,” *Color Research and Application* 30, no. 1 (2005): 21–30.
13. C. Li, Z. Li, Z. Wang, et al., “A Revision of CIECAM02 and Its CAT and UCS,” in *Color and Imaging Conference*, vol. 2016, no. 1 (Springfield, Illinois: Society for Imaging Science and Technology, 2016), 208–212.
14. C. Li, Z. Li, Z. Wang, et al., “Comprehensive Color Solutions: CAM16, CAT16, and CAM16-UCS,” *Color Research and Application* 42, no. 6 (2017): 703–718.
15. Y. Nayatani, K. Takahama, and H. Sobagaki, “Prediction of Color Appearance Under Various Adapting Conditions,” *Color Research and Application* 11 (1986): 62–71.
16. R. W. G. Hunt, “A Model of Colour Vision for Predicting Colour Appearance,” *Color Research and Application* 7 (1982): 95–112.

17. M. D. Fairchild, "Refinement of the RLAB Color Space," *Color Research and Application* 21 (1996): 338–346.
18. CIE, *The CIE 1997 Interim Colour Appearance Model (Simple Version)*, CIECAM97s, vol. 131 (Vienna: CIE Publications, 1998).
19. CIE, *CIE TC8-01 Technical Report, A Colour Appearance Model for Color Management Systems: CIECAM02*, vol. 159 (Vienna: CIE Publications, 2004).
20. M. R. Luo, G. Cui, and C. Li, "Uniform Colour Spaces Based on CIECAM02 Colour Appearance Model," *Color Research & Application* Endorsed by Inter-Society Color Council, The Colour Group (Great Britain), Canadian Society for Color, Color Science Association of Japan, Dutch Society for the Study of Color, The Swedish Colour Centre Foundation, Colour Society of Australia, Centre Français de la Couleur 31, no. 4 (2006): 320–330.
21. B. V. Funt and E. Roshan, "Metamer Mismatching Underlies Color Difference Sensitivity," *Journal of Vision* 21, no. 12 (2021): 1–11.
22. D. L. MacAdam, "Visual Sensitivities to Color Differences in Daylight," *Journal of the Optical Society of America* 32, no. 5 (1942): 247–274.
23. M. Mahy, L. van Eycken, and A. Oosterlinck, "Evaluation of Uniform Color Spaces Developed After the Adoption of CIELAB and CIELUV," *Color Research and Application* 19, no. 2 (1994): 105–121.
24. F. Martín, J. Valls Miró, and L. Moreno, "Towards Exploiting the Advantages of Colour in Scan Matching," in *ROBOT2013: First Iberian Robotics Conference* (Cham: Springer, 2014), 217–231.
25. L. Hao, J. Feng, and B. Zhou, "Gradient Domain Binary Image Hiding Using Color Difference Metric," in *SIGGRAPH Asia 2015 Technical Briefs* (New York: Association for Computing Machinery, 2015), 1–4.
26. Y. Zhang, R. Wang, E. Y. Peng, W. Hua, and H. Bao, "Color Contrast Enhanced Rendering for Optical See-Through Head-Mounted Displays," *IEEE Transactions on Visualization and Computer Graphics* 28 (2021): 4490–4502.
27. E. Roshan and B. Funt, "Color Sensor Accuracy Index Utilizing Metamer Mismatch Radii," *Sensors* 20, no. 15 (2020): 4275.
28. A. D. Logvinenko, B. Funt, and C. Godau, "Metamer Mismatching," *IEEE Transactions on Image Processing* 23, no. 1 (2013): 34–43.
29. R. S. Berns, D. H. Alman, L. Reniff, G. D. Snyder, and M. R. Balonon-Rosen, "Visual Determination of Suprathreshold Color-Difference Tolerances Using Probit Analysis," *Color Research & Application* 16, no. 5 (1991): 297–316.
30. W. R. J. Brown and D. L. MacAdam, "Visual Sensitivities to Combined Chromaticity and Luminance Differences," *Journal of the Optical Society of America* 39, no. 10 (1949): 808–834.
31. A. D. Logvinenko, "An Object-Color Space," *Journal of Vision* 9 (2009): 1–23.
32. M. Moshtaghi, T. C. Havens, J. C. Bezdek, et al., "Clustering Ellipses for Anomaly Detection," *Pattern Recognition* 44, no. 1 (2011): 55–69.
33. E. A. Merritt, "Comparing Anisotropic Displacement Parameters in Protein Structures," *Acta Crystallographica Section D: Biological Crystallography* 55, no. 12 (1999): 1997–2004.
34. M. Melgosa, E. Hita, A. Poza, D. H. Alman, and R. S. Berns, "Suprathreshold Color-Difference Ellipsoids for Surface Colors," *Color Research & Application* 22, no. 3 (1997): 148–155.
35. A. R. Robertson, "Guidelines for Coordinated Research on Colour Difference Equations," *Color Research & Application* 3 (1978): 149–151.
36. K. Witt, "Three-Dimensional Threshold of Color-Difference Perceptibility in Painted Samples: Variability of Observers in Four CIE Color Regions," *Color Research & Application* 12, no. 3 (1987): 128–134.
37. M. Cheung and B. Rigg, "Colour-difference ellipsoids for five CIE colour centres," *Color Research & Application* 11, no. 3 (1986): 185–195.
38. M. Huang, H. Liu, G. Cui, and M. R. Luo, "Testing Uniform Colour Spaces and Colour-Difference Formulae Using Printed Samples," *Color Research & Application* 37, no. 5 (2012): 326–335.
39. X. Zhang, B. Funt, and H. Mirzaei, "Metamer Mismatching in Practice Versus Theory," *Journal of the Optical Society of America A* 33, no. 3 (2016): A238–A247.